Yttrium Doped Barium Fluoride Crystals for Future HEP Experiments

Ren-Yuan Zhu

California Institute of Technology

August 20, 2018

Why Ultrafast Crystals?

- Photons and electrons are fundamental particles. Precision e/γ measurements enhance physics discovery potential.
- Performance of crystal calorimeter in e/γ measurements is well understood:
  - The best possible energy resolution;
  - Good position resolution;
  - Good e/γ identification and reconstruction efficiency.
- Challenges at future HEP & other applications:
  - Ultrafast and rad hard crystals at the energy frontier (HL-LHC);
  - Ultrafast crystals at the intensity frontier (Mu2e-II);
  - Ultrafast crystals for GHz hard X-ray imaging (Marie).

Application of Ultrafast Crystals

Ultrafast and radiation hard inorganic scintillators have broad applications

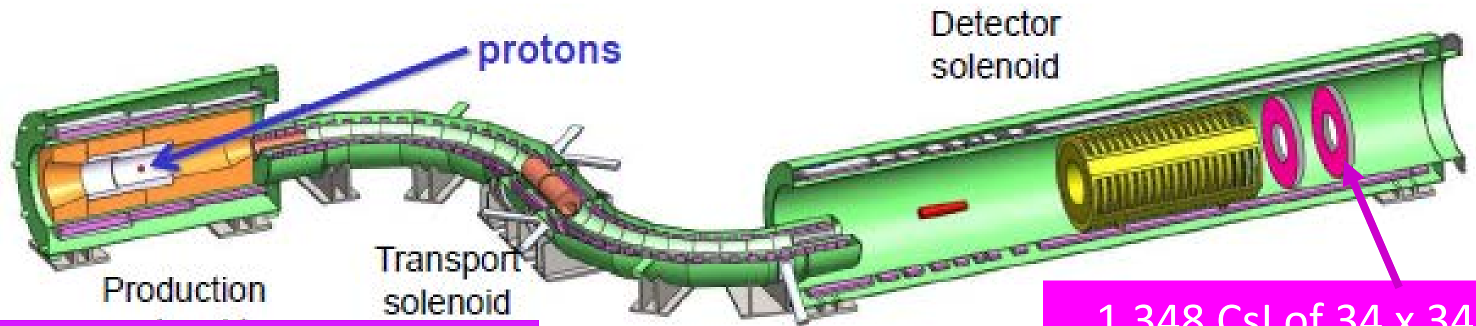

Mu2e-II: arXiv:1802.02599

1,348 CsI of 34 x 34 x 200 mm
1940 BaF_2:Y of 30 x 30 x 218 mm

BaF_2:Y, and other ultrafast crystals are attractive for an ultrafast front imager for GHz hard x-ray imaging

Marie Project

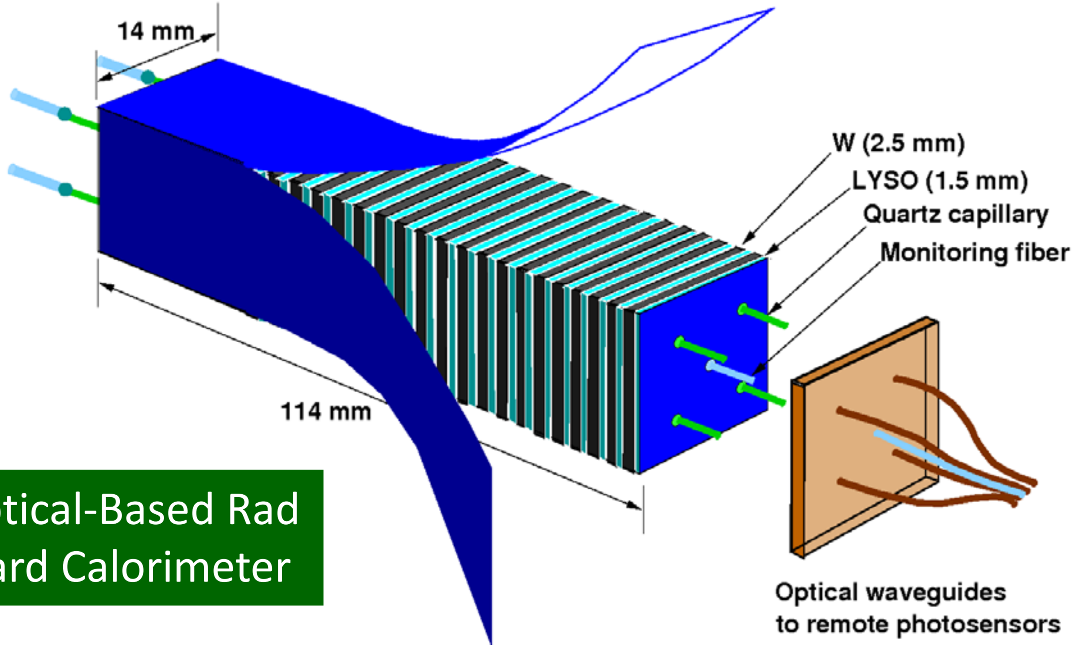

Optical-Based Rad Hard Calorimeter

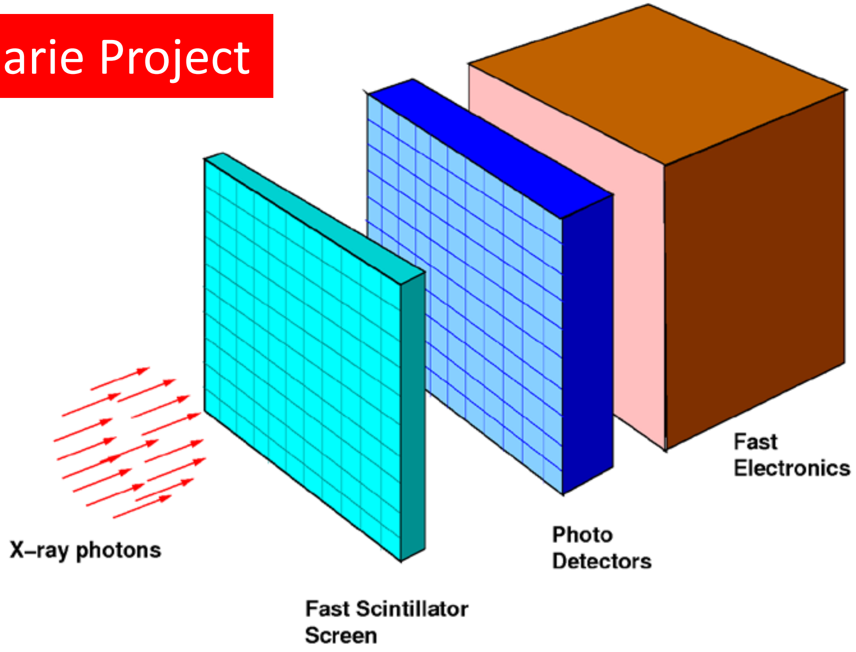

GHz Hard X-Ray Imaging for Marie

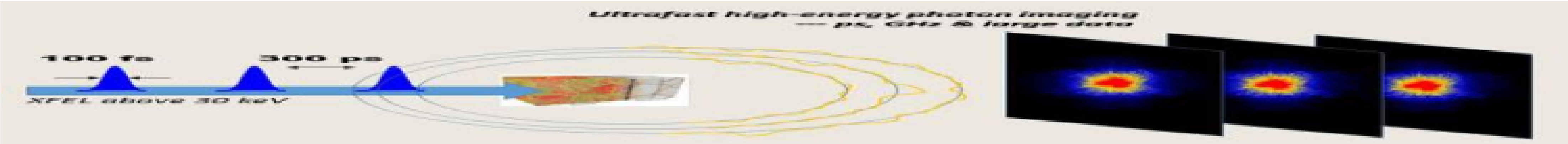

High-Energy and Ultrafast X-Ray Imaging Technologies and Applications

Organizers: Peter Denes, Sol Gruner, Michael Stevens & Zhehui (Jeff) Wang[1]
*(**Location/Time**: Santa Fe, NM, USA /Aug 2-3, 2016)*

The goals of this workshop are to gather the leading experts in the related fields, to prioritize tasks for ultrafast hard X-ray imaging detector technology development and applications in the next 5 to 10 years, see Table 1, and to establish the foundations for near-term R&D collaborations.

Table I. High-energy photon imagers for MaRIE XFEL

Performance	Type I imager	Type II imager
X-ray energy	30 keV	42-126 keV
Frame-rate/inter-frame time	0.5 GHz/2 ns	3 GHz / 300 ps
Number of frames	10	10 - 30
X-ray detection efficiency	above 50%	above 80%
Pixel size/pitch	≤ 300 μm	< 300 μm
Dynamic range	10^3 X-ray photons	≥ 10^4 X-ray photons
Pixel format	64 x 64 (scalable to 1 Mpix)	1 Mpix

2 ns and 300 ps inter-frame time requires very fast sensor

Fast and Ultrafast Inorganic Scintillators

	BaF_2	BaF_2:Y	ZnO:Ga	YAP:Yb	YAG:Yb	β-Ga_2O_3	LYSO:Ce	LuAG:Ce	YAP:Ce	GAGG:Ce	LuYAP:Ce	YSO:Ce
Density (g/cm^3)	4.89	4.89	5.67	5.35	4.56	5.94[1]	7.4	6.76	5.35	6.5	7.2[f]	4.44
Melting points (^{o}C)	1280	1280	1975	1870	1940	1725	2050	2060	1870	1850	1930	2070
X_0 (cm)	2.03	2.03	2.51	2.77	3.53	2.51	1.14	1.45	2.77	1.63	1.37	3.10
R_M (cm)	3.1	3.1	2.28	2.4	2.76	2.20	2.07	2.15	2.4	2.20	2.01	2.93
λ_I (cm)	30.7	30.7	22.2	22.4	25.2	20.9	20.9	20.6	22.4	21.5	19.5	27.8
Z_{eff}	51.6	51.6	27.7	31.9	30	28.1	64.8	60.3	31.9	51.8	58.6	33.3
dE/dX (MeV/cm)	6.52	6.52	8.42	8.05	7.01	8.82	9.55	9.22	8.05	8.96	9.82	6.57
λ_{peak}[a] (nm)	300 220	300 220	380	350	350	380	420	520	370	540	385	420
Refractive Index[b]	1.50	1.50	2.1	1.96	1.87	1.97	1.82	1.84	1.96	1.92	1.94	1.78
Normalized Light Yield[a,c]	42 4.8	1.7 4.8	6.6[d]	0.19[d]	0.36[d]	6.5 0.5	100	35[e] 48[e]	9 32	115	16 15	80
Total Light yield (ph/MeV)	13,000	2,000	2,000[d]	57[d]	110[d]	2,100	30,000	25,000[e]	12,000	34,400	10,000	24,000
Decay time[a] (ns)	600 0.6	600 0.6	<1	1.5	4	148 6	40	820 50	191 25	53	1485 36	75
LY in 1st ns (photons/MeV)	1200	1200	610[d]	28[d]	24[d]	43	740	240	391	640	125	318
40 keV Att. Leng. (1/e, mm)	0.106	0.106	0.407	0.314	0.439	0.394	0.185	0.251	0.314	0.319	0.214	0.334

Ultrafast and Slow Light from BaF_2

BaF_2 has a fast scintillation component with sub-ns decay time, and a 600 ns slow component.

The amount of the fast light is similar to undoped CsI, and is 1/5 of the slow component.

Spectroscopic readout of the fast component may be realized by selective doping with rare earths and/or a solar blind photodetector.

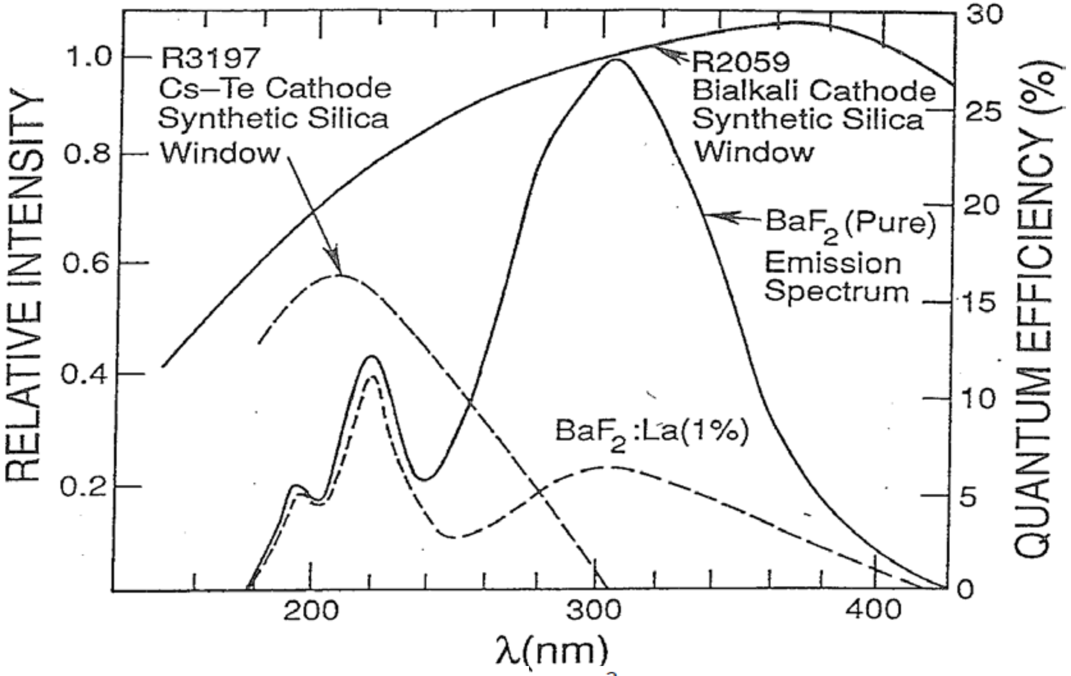

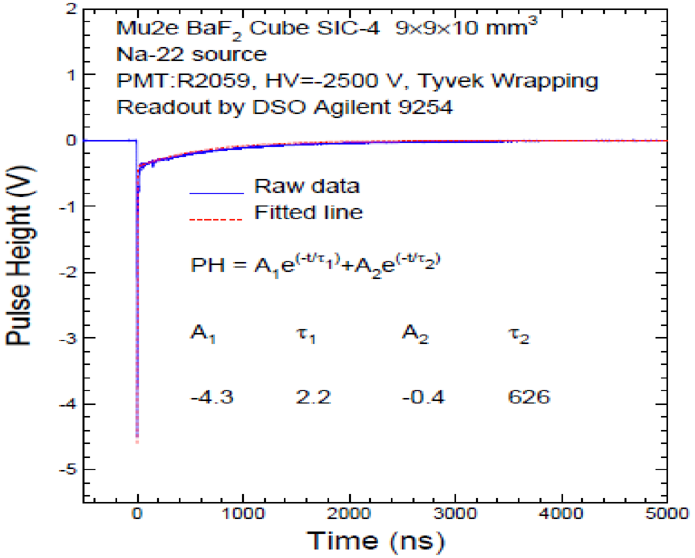

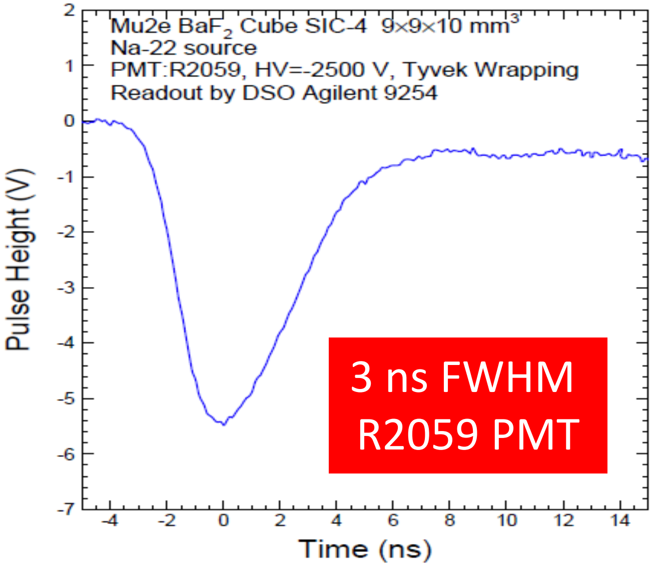

3 ns FWHM
R2059 PMT

Slow Suppression: Doping & Readout

Slow component may be suppressed by RE doping: Y, La and Ce

B.P. SOBOLEV et al., "SUPPRESSION OF BaF2 SLOW COMPONENT OF X-RAY LUMINESCENCE IN NON-STOICHIOMETRIC Ba0.9R0.1F2 CRYSTALS (R=RARE EARTH ELEMENT)," *Proceedings of The Material Research Society: Scintillator and Phosphor Materials*, pp. 277-283, 1994.

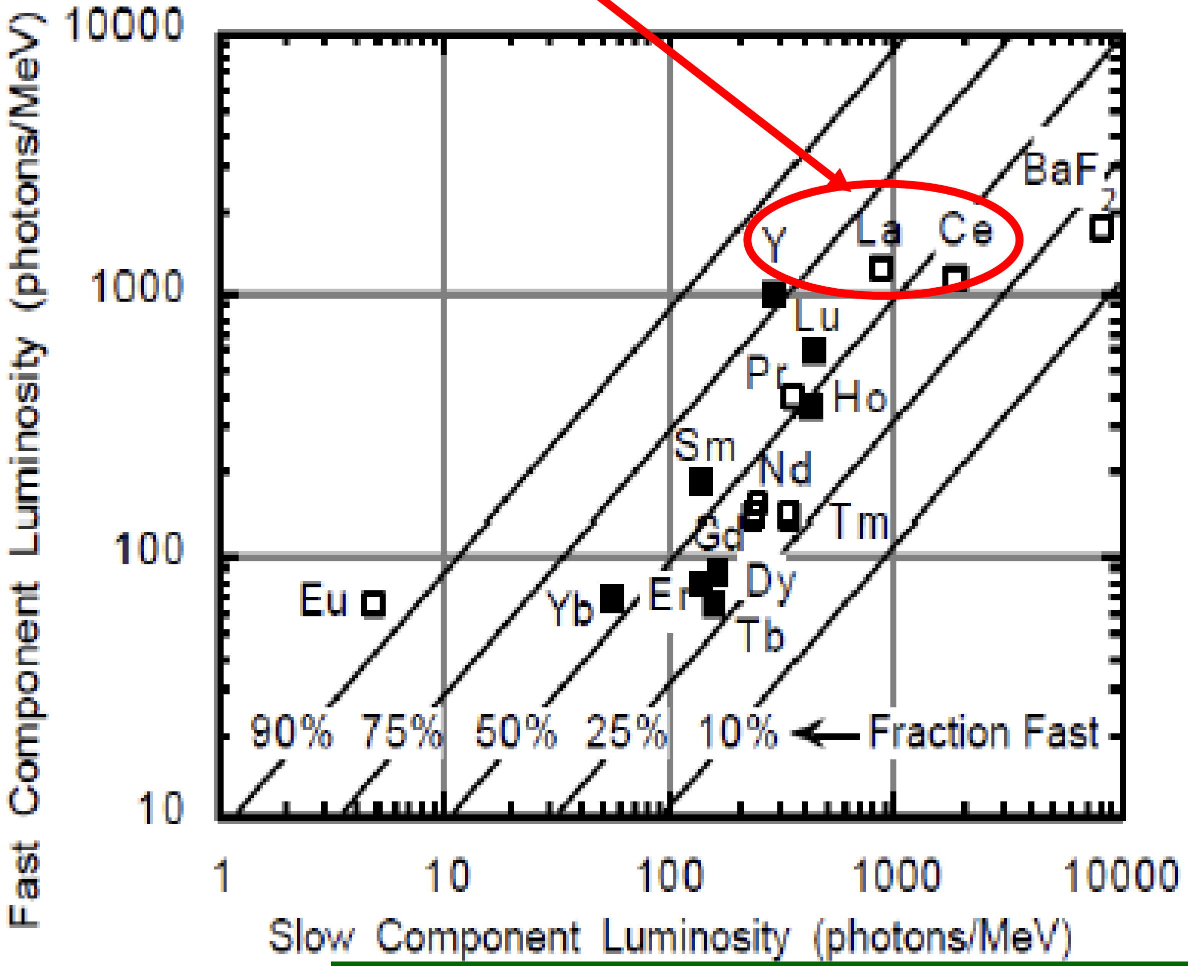

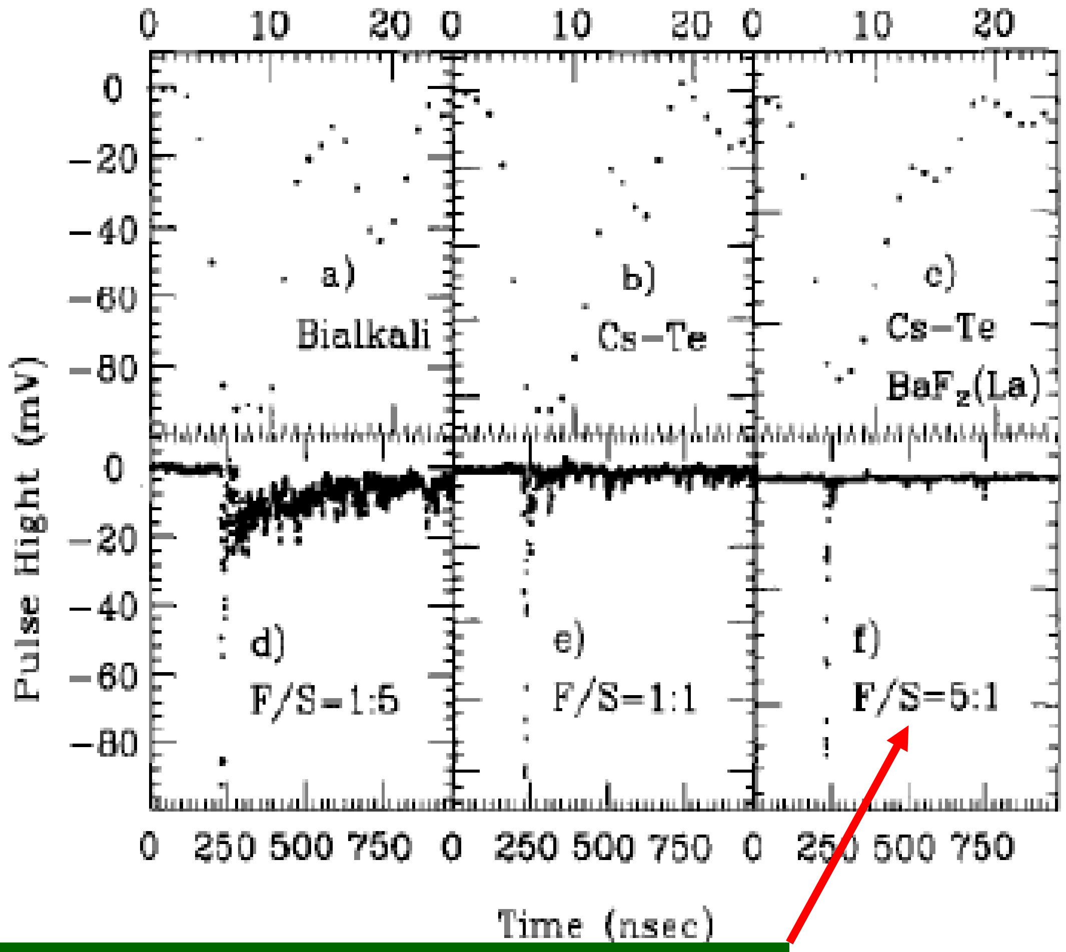

Solar-blind cathode (Cs-Te) and La doping achieved F/S = 5/1

Yttrium Doped BaF_2

Sub-ns FWHM by MCP-PMT; Significant increase in F/S ratio by BaF_2:Y

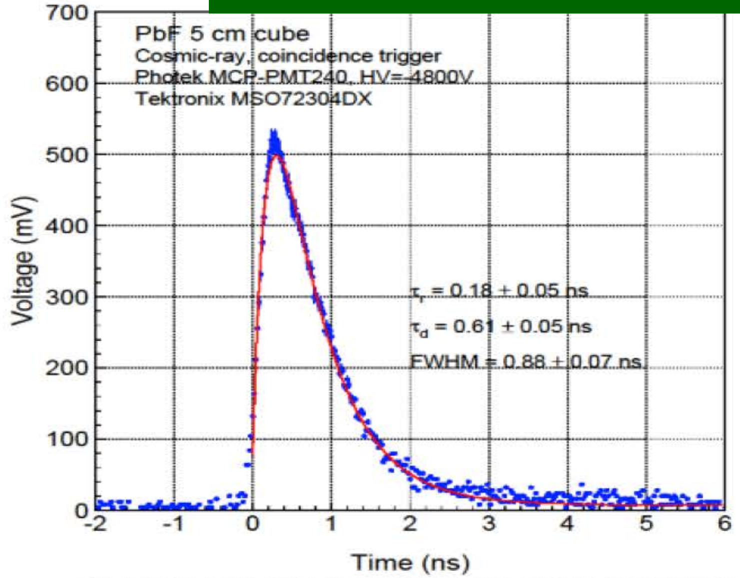

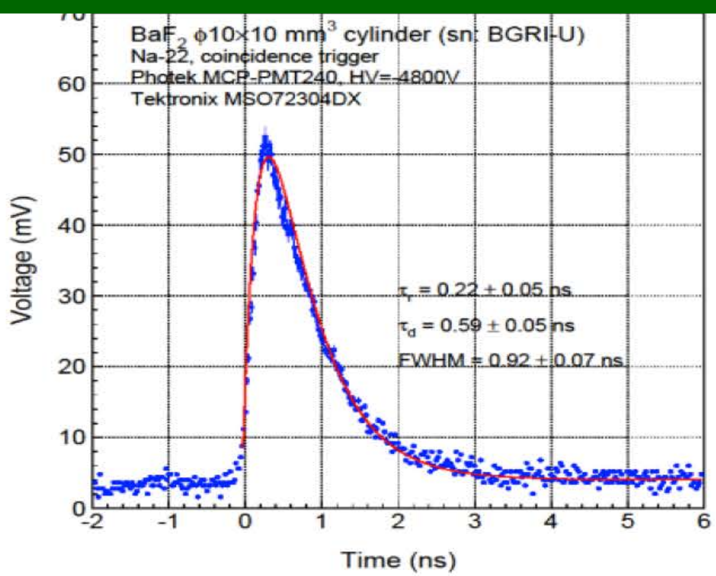

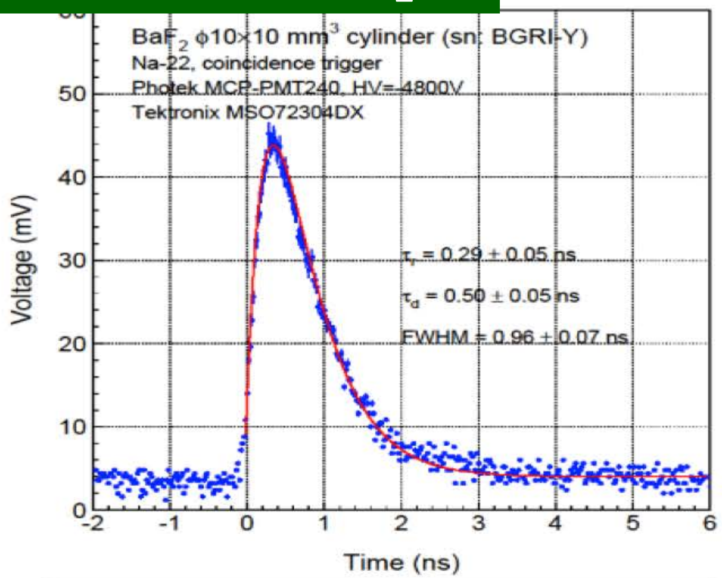

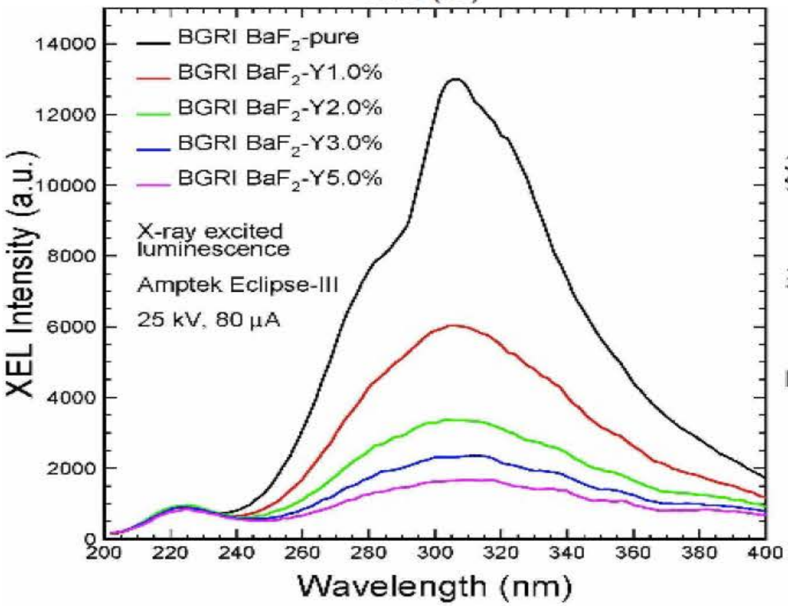

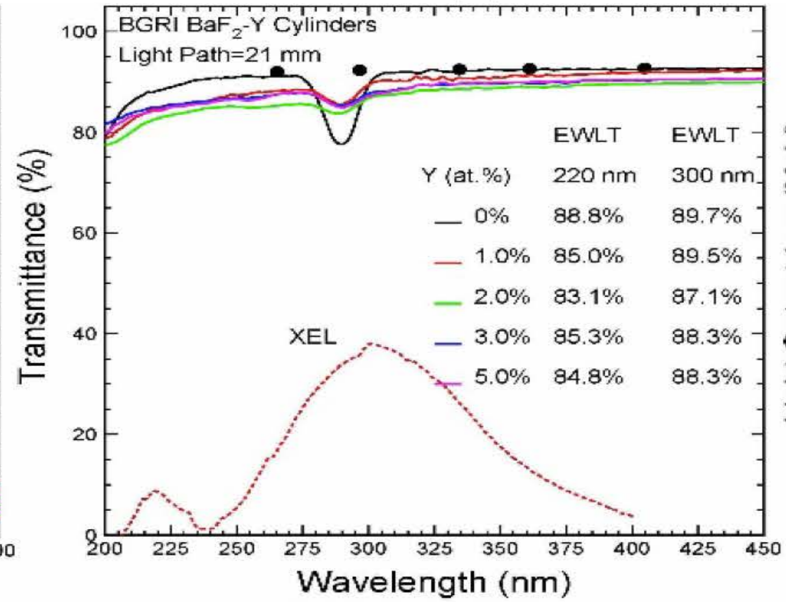

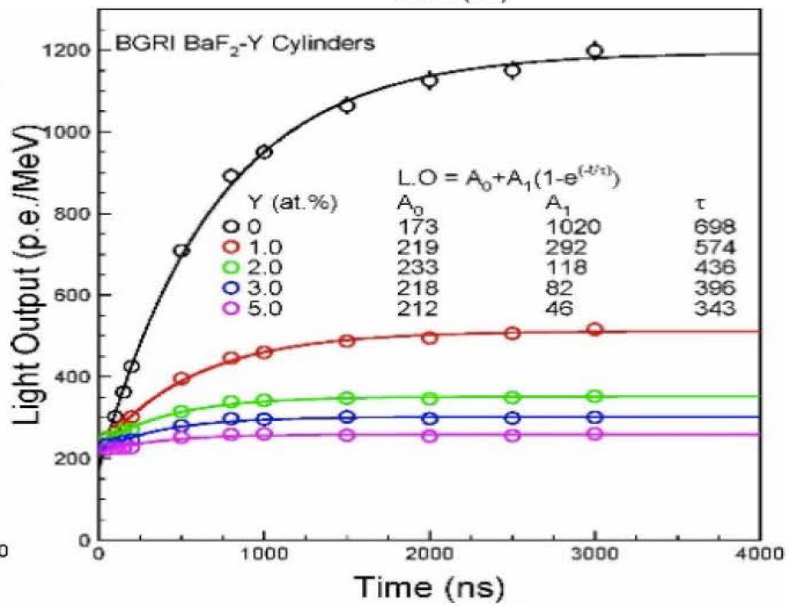

Fast Inorganic Scintillators Tested at APS

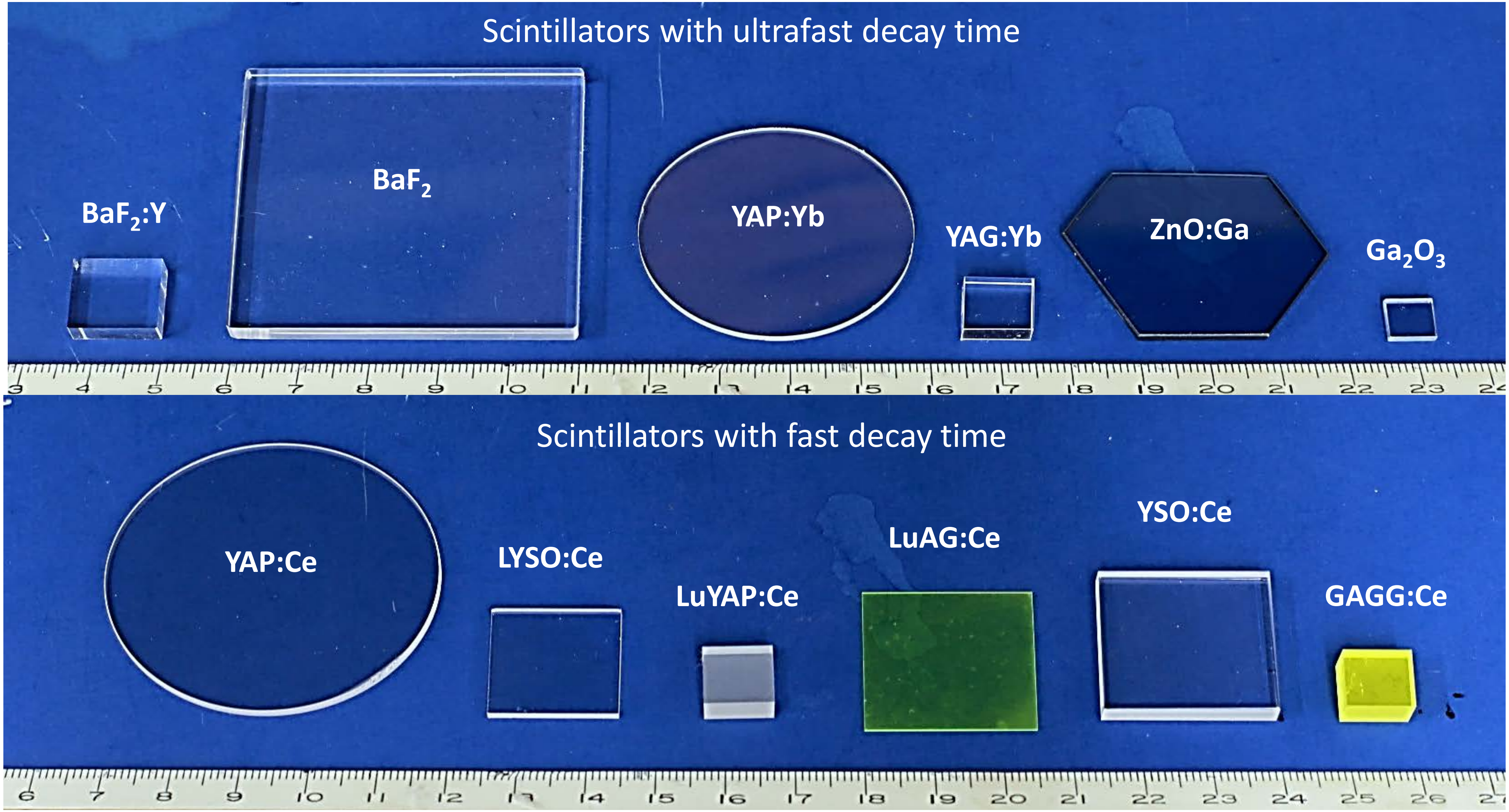

Test Setup at Advanced Photon Source

Crystals, MCP-PMT and gate unit were in the hutch at APS 10-ID site; DPO, delay generator and HV power supplier were in the control room; Signal from MCP-PMT went through a 15 m wideband SMA cable.

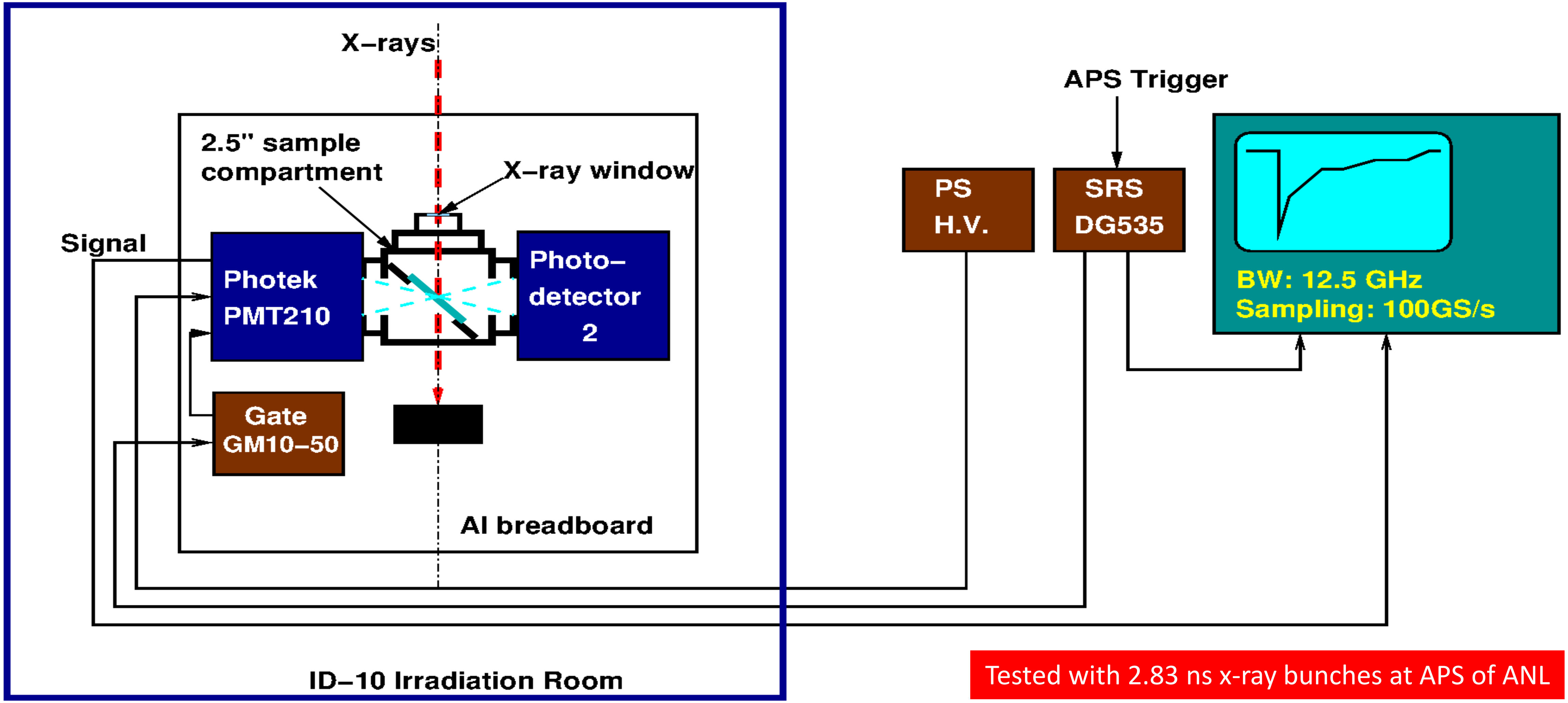

Tested with 2.83 ns x-ray bunches at APS of ANL

APS Hybrid Beam Characteristics

Singlet (16 mA, 50 ps) isolated from 8 septuplets (88 mA) with 1.594 µs gap; 8 septuplets (88 mA) with a period of 68 ns and a gap of 51 ns; Each septuplet of 17 ns consists of 7 bunches (27 ps) and 2.83 ns apart; Total beam current: 102 mA, rate: 270 kHz, period: 3.7 µs.

https://ops.aps.anl.gov/SRparameters/node5.html

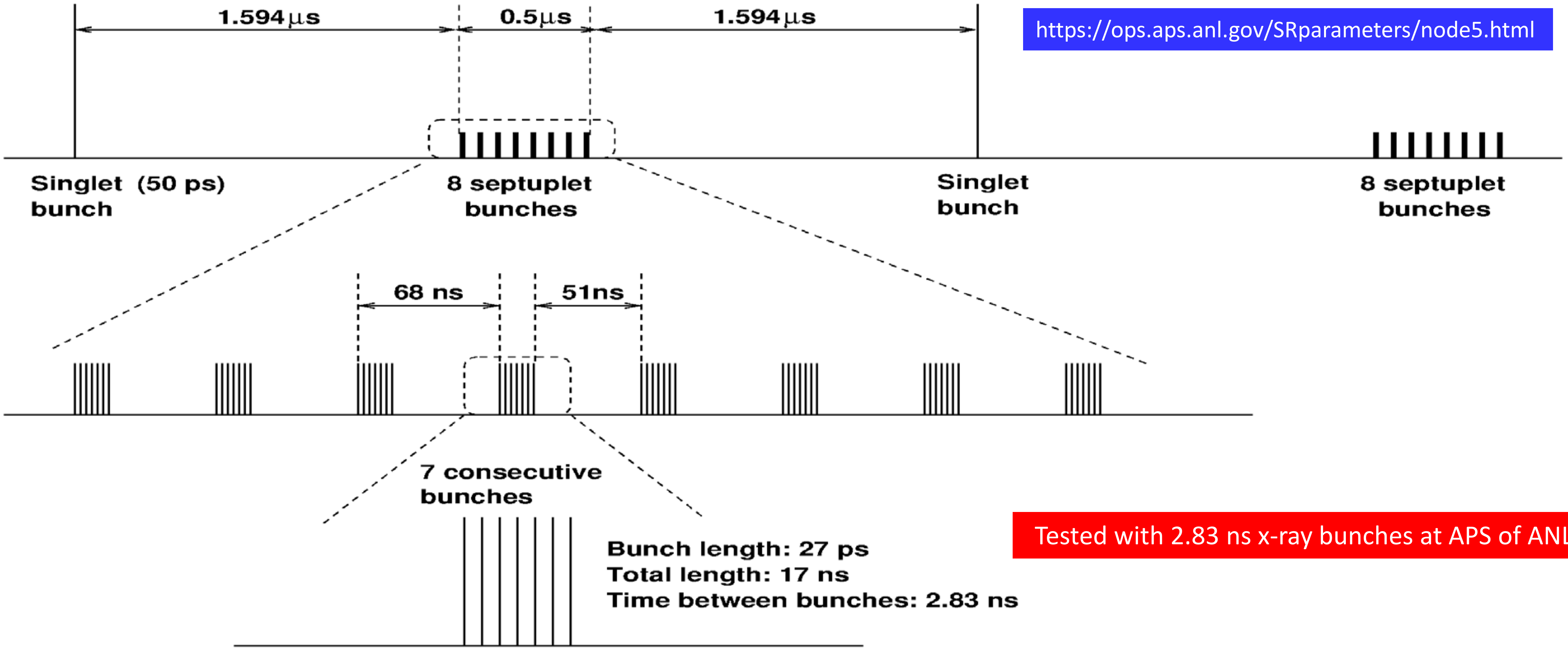

Tested with 2.83 ns x-ray bunches at APS of ANL

Hybrid Beam Measured by BaF_2:Y

Data were taken with Photek PMT & gate unit for septuplet bunches to see crystal's capability for hard X-ray imaging with 2.83 ns bunch spacing.

Data were also taken for singlet bunches to measure crystal's temporal response.

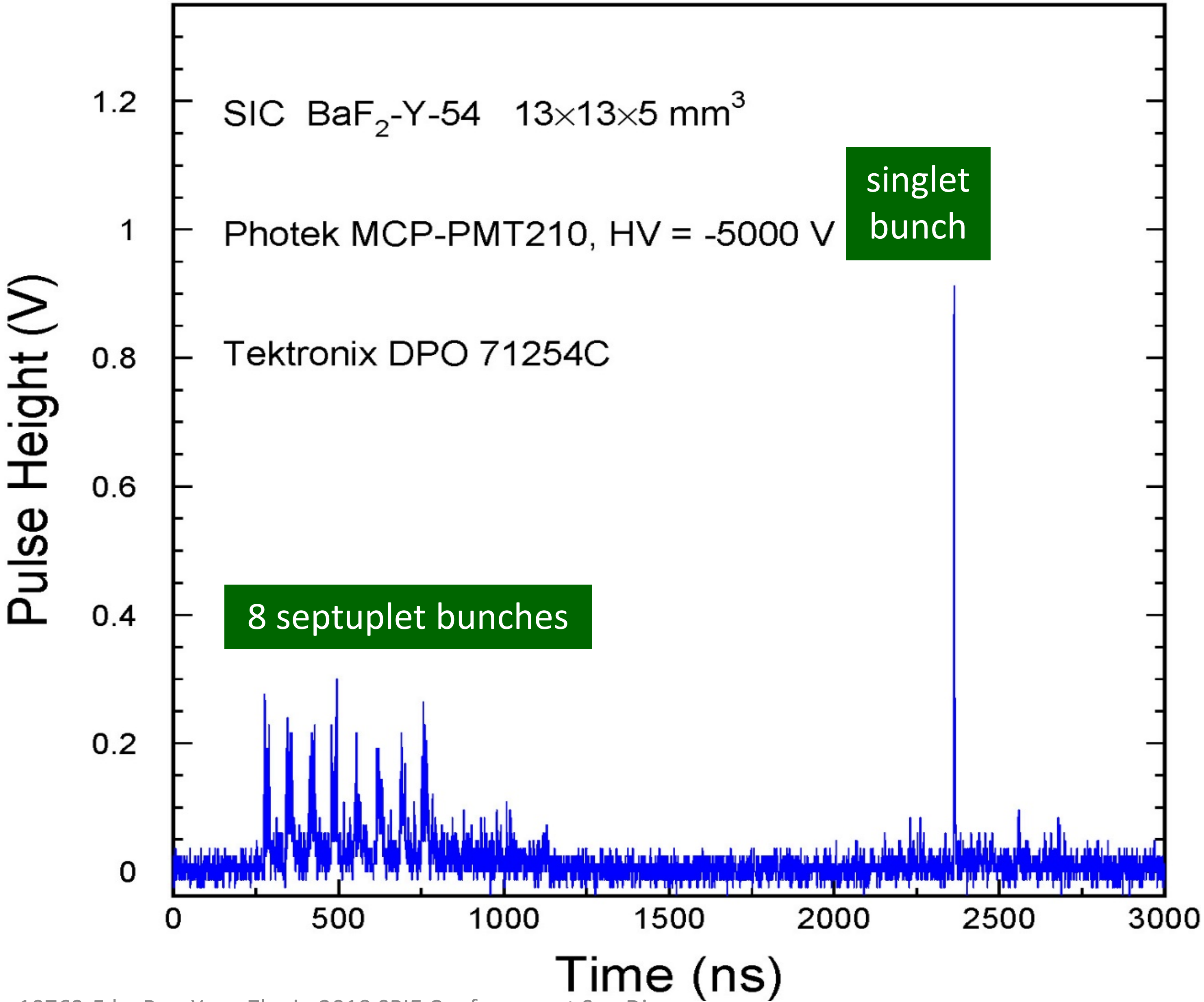

X-ray Imaging for Septuplet

Clear septuplet structure observed by BaF_2:Y, BaF_2 and ZnO:Ga, but not by LYSO:Ce and others

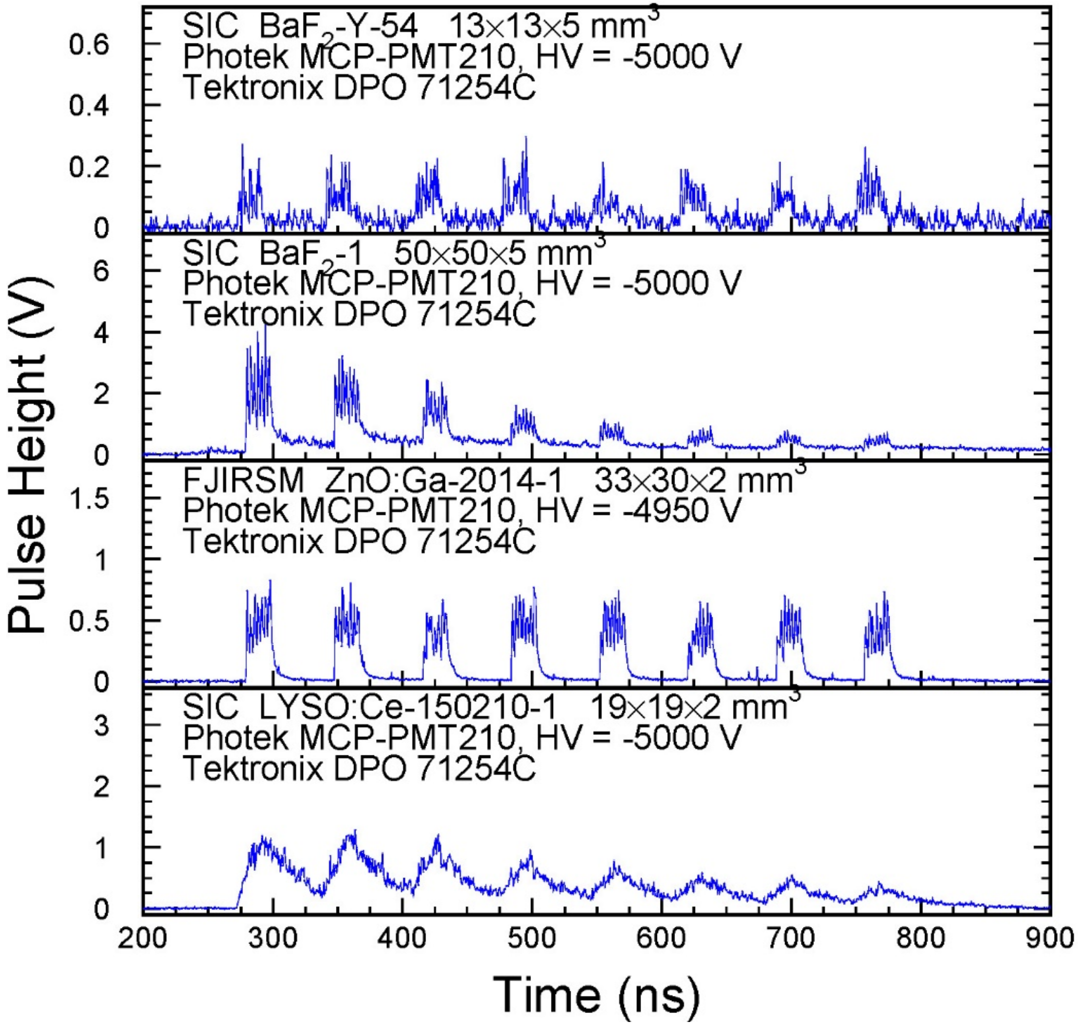

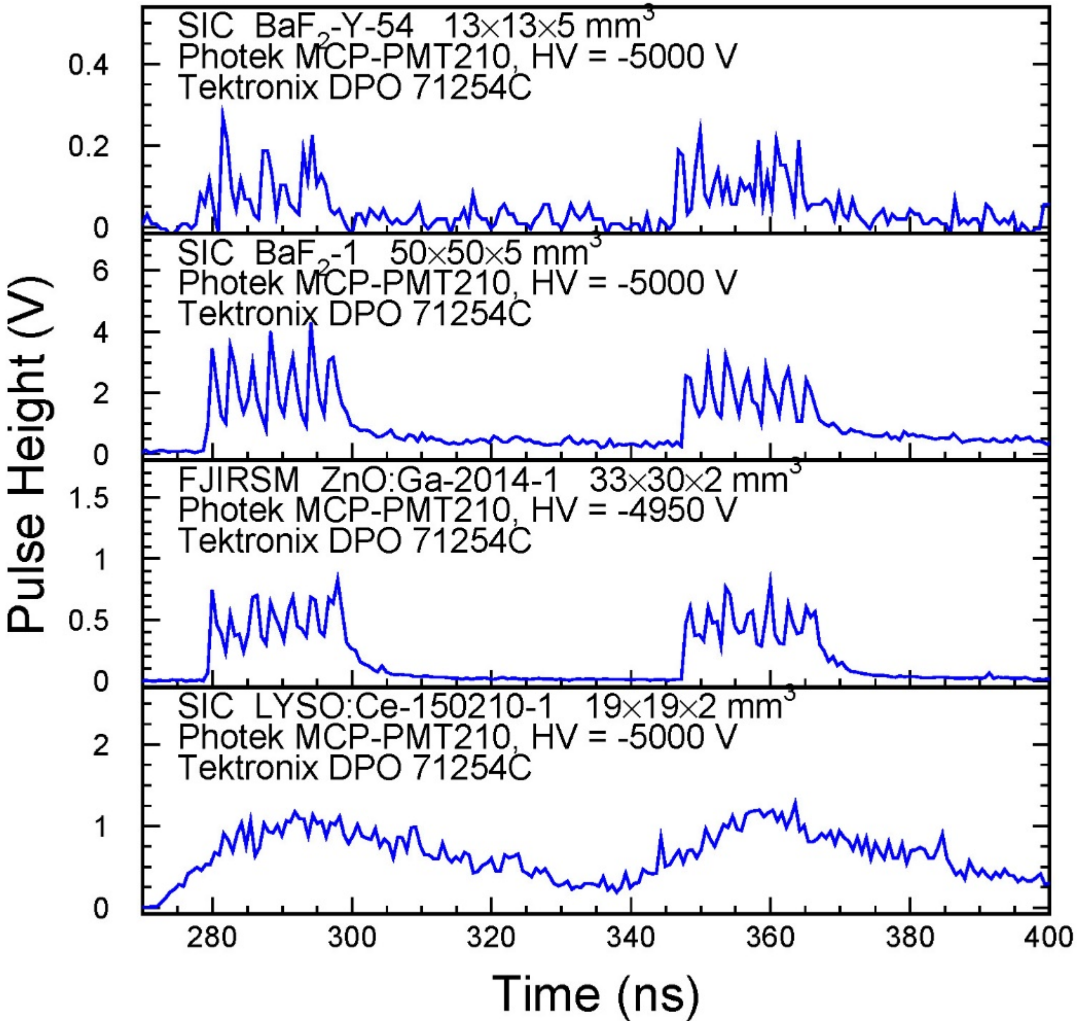

Amplitude reduction for septuplets in BaF_2 and LYSO, but not BaF_2:Y, due to space charge in PMT from slow scintillation

2.83 ns X-ray Bunch Imaging by BaF_2

X-ray bunches with 2.83 ns spacing in septuplet are clearly resolved by ultrafast BaF_2 crystals, showing a proof-of-principle for the type –I imager.

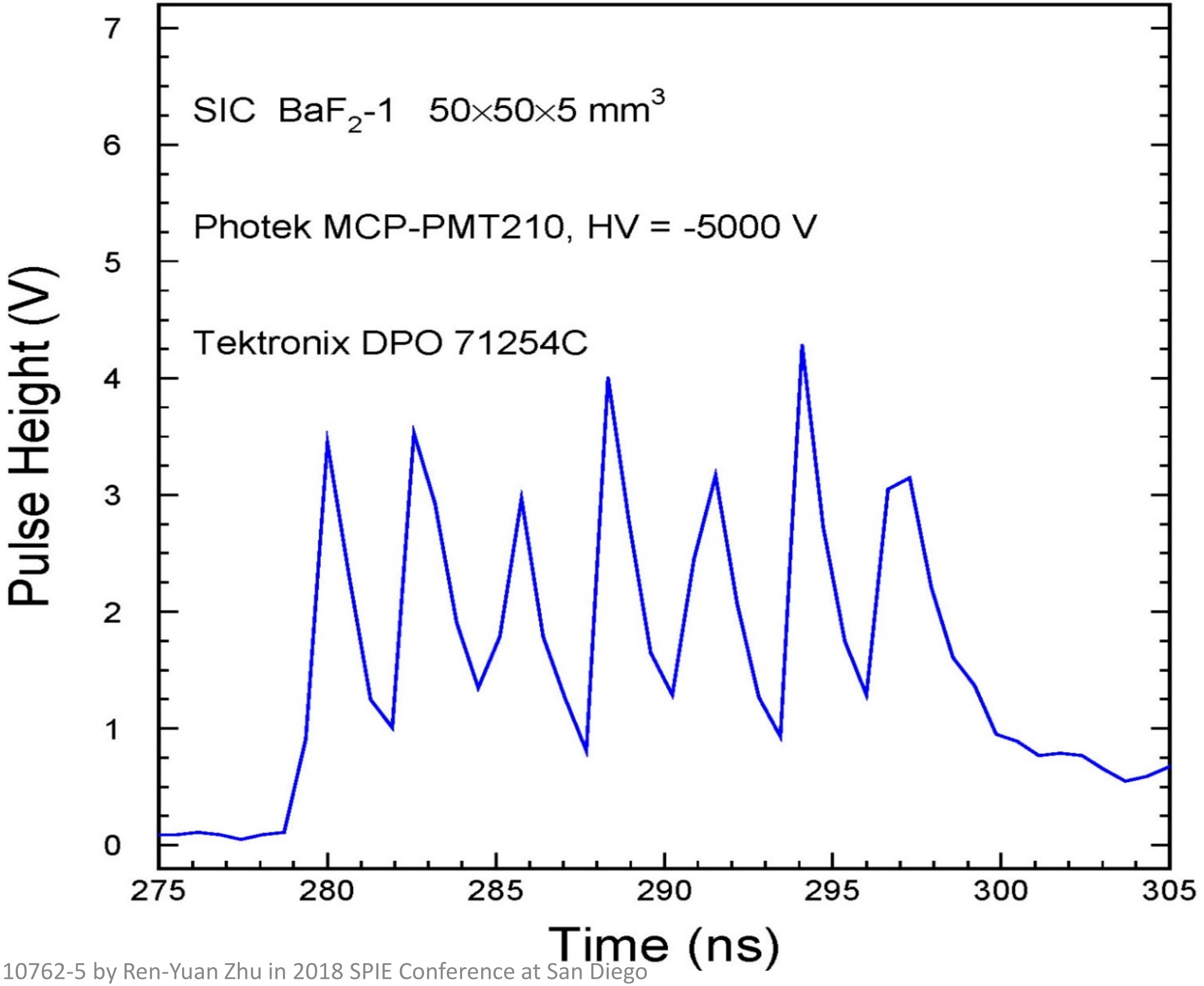

Singlet Bunch by Ultrafast Crystals

Peak of BaF_2 and BaF_2:Y higher than ZnO:Ga and LYSO; Decay of BaF_2 and BaF_2:Y shorter than ZnO:Ga.

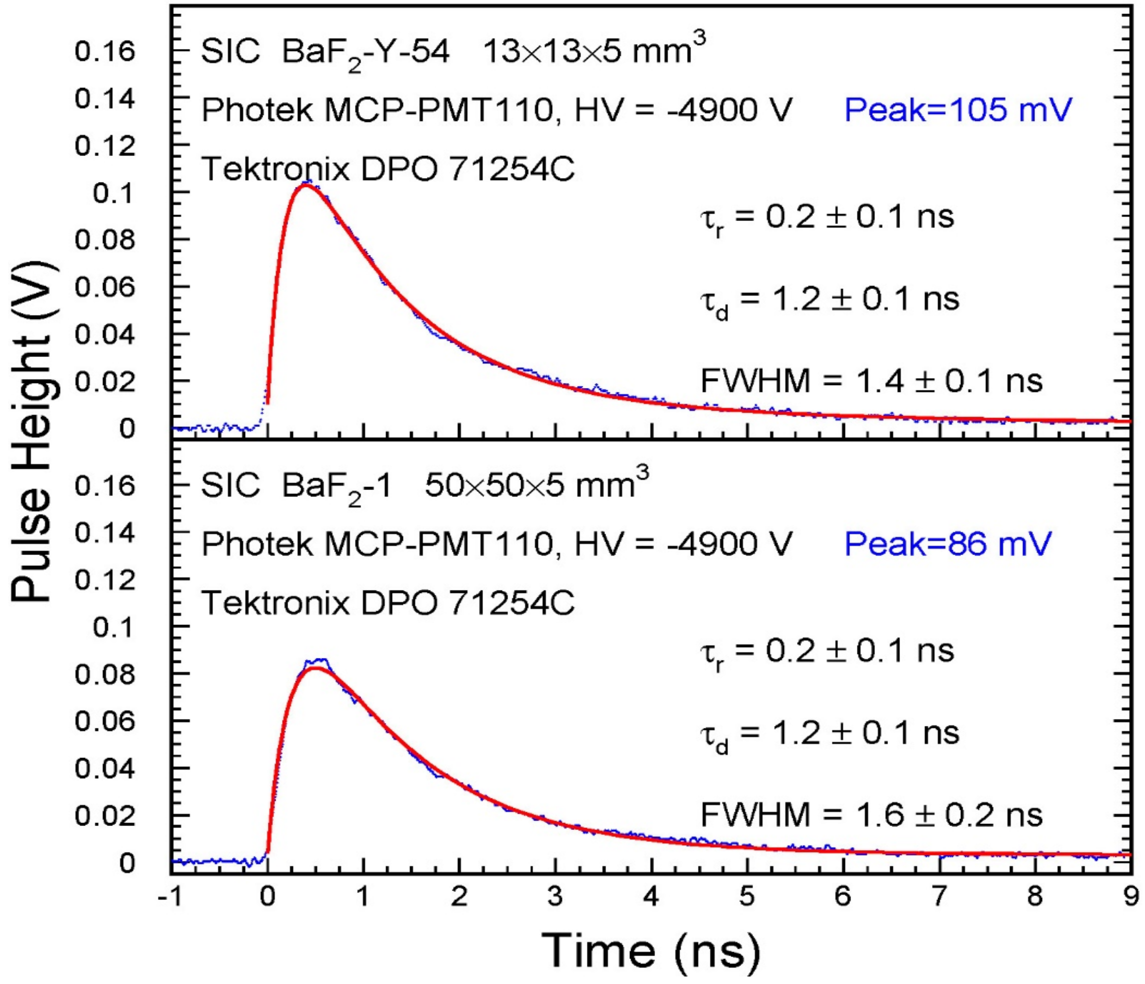

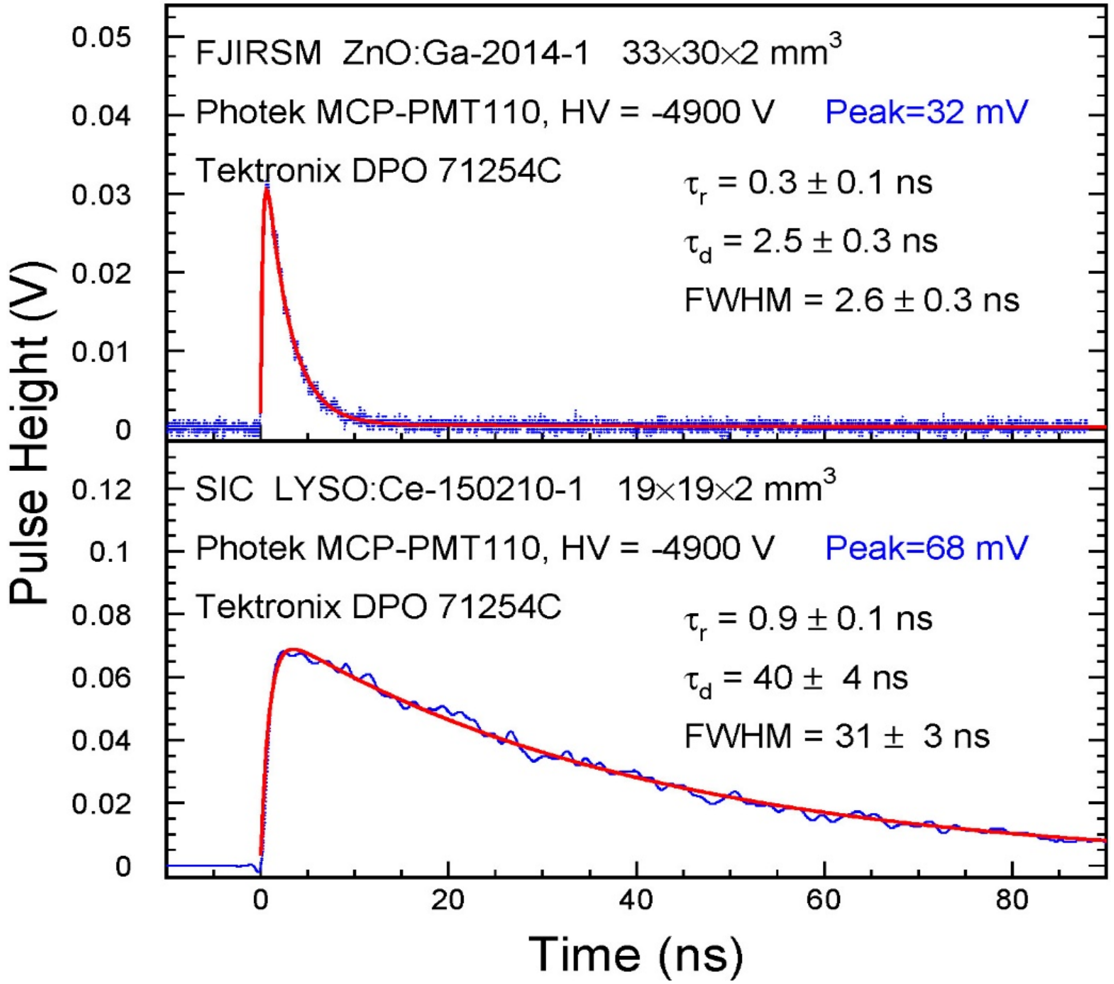

Rise and decay time of BaF_2 and BaF_2:Y longer than the ɣ-ray response due to the 15 m cable

γ-Ray Induced Damage in Large Samples

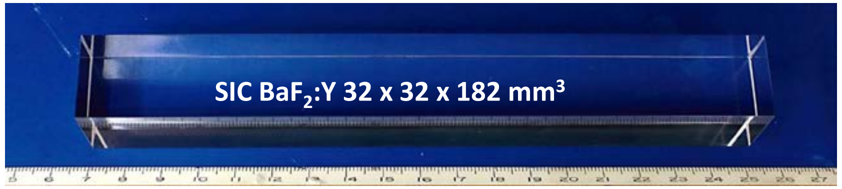

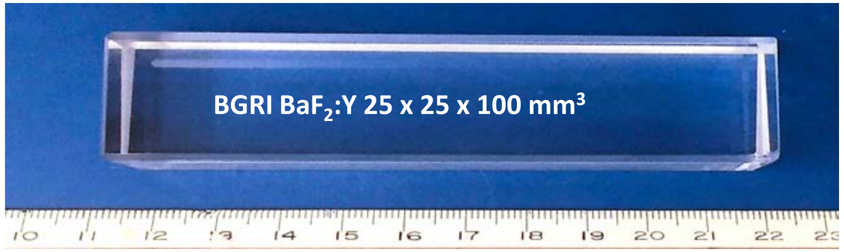

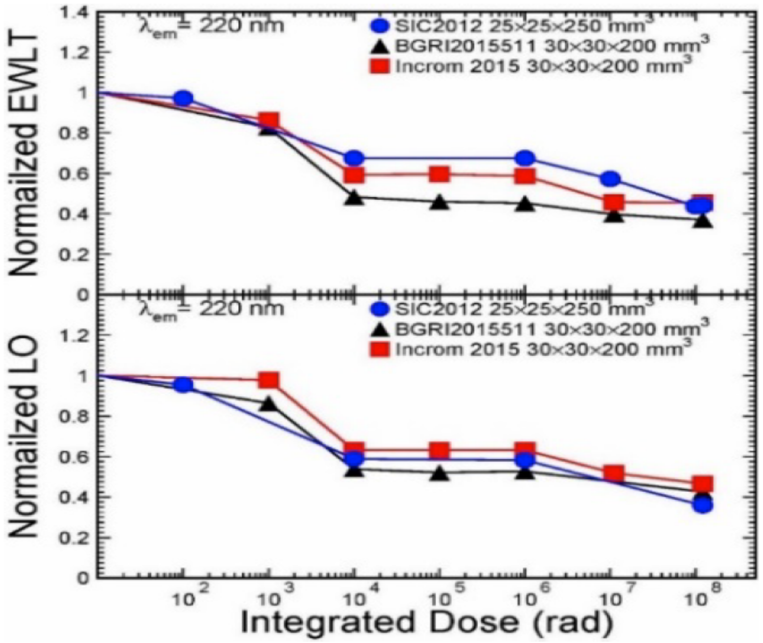

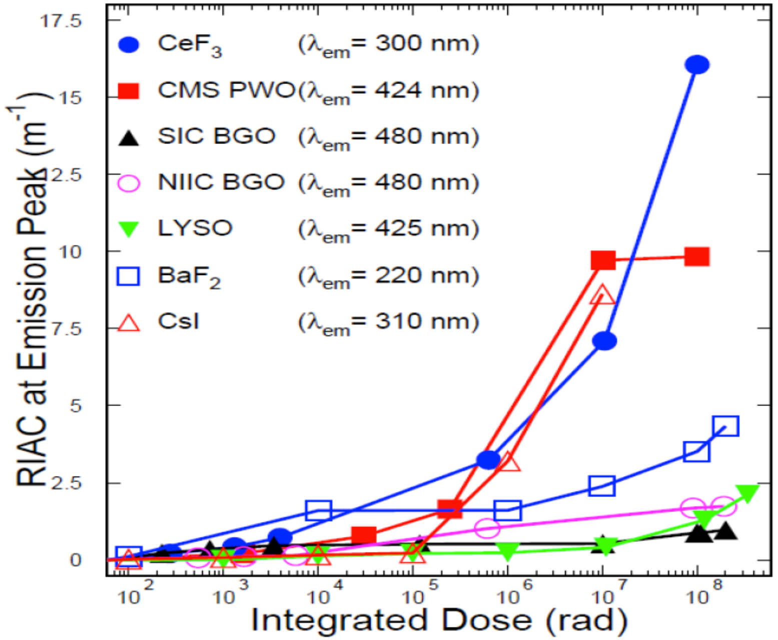

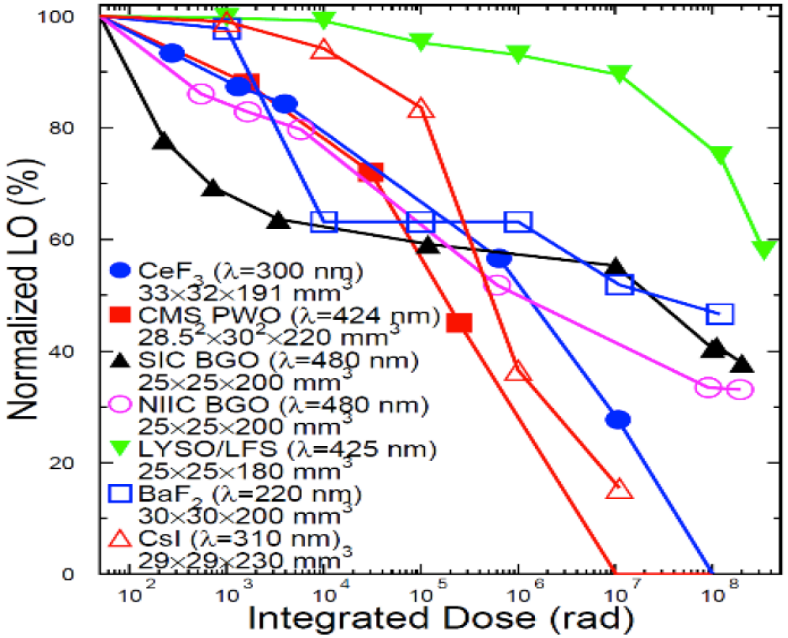

Proton and Neutron Induced Damage

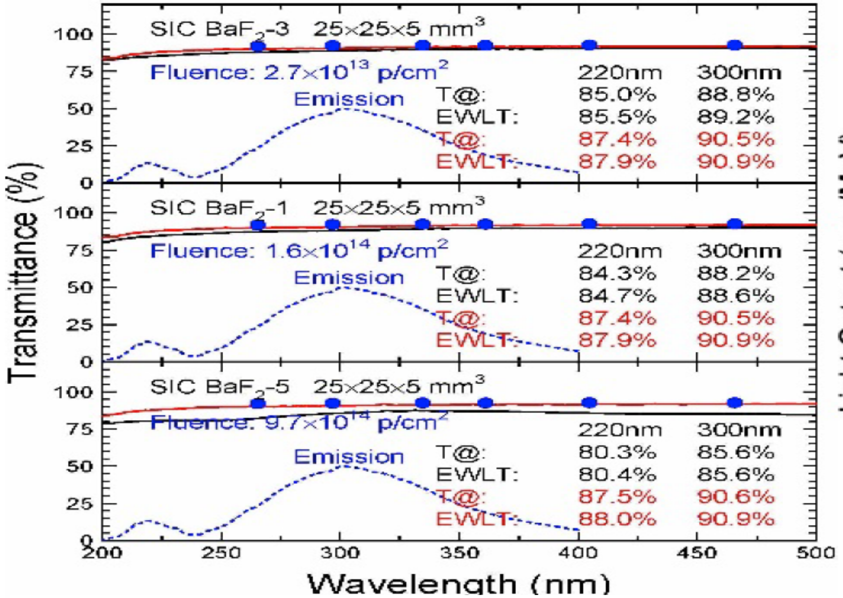

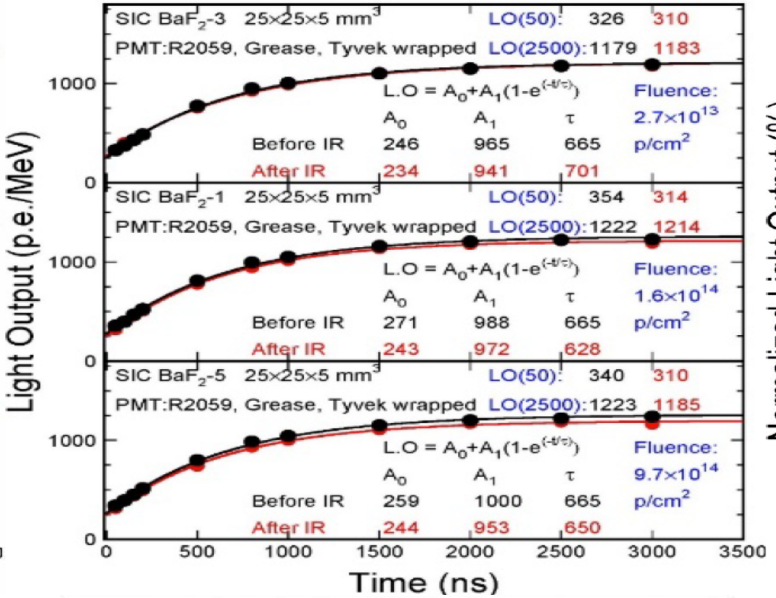

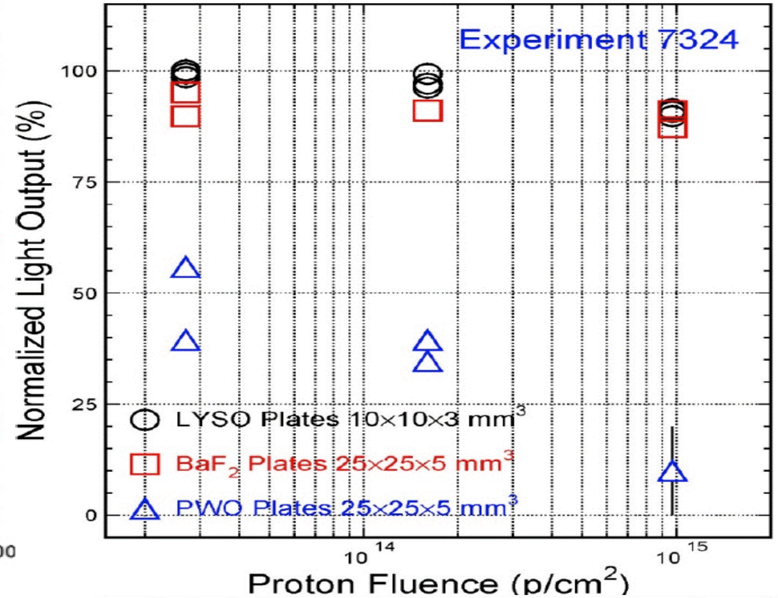

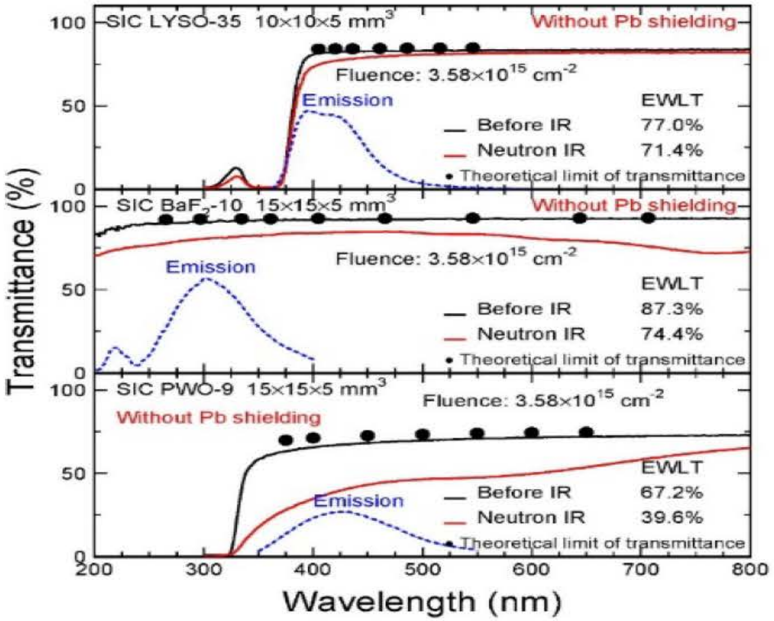

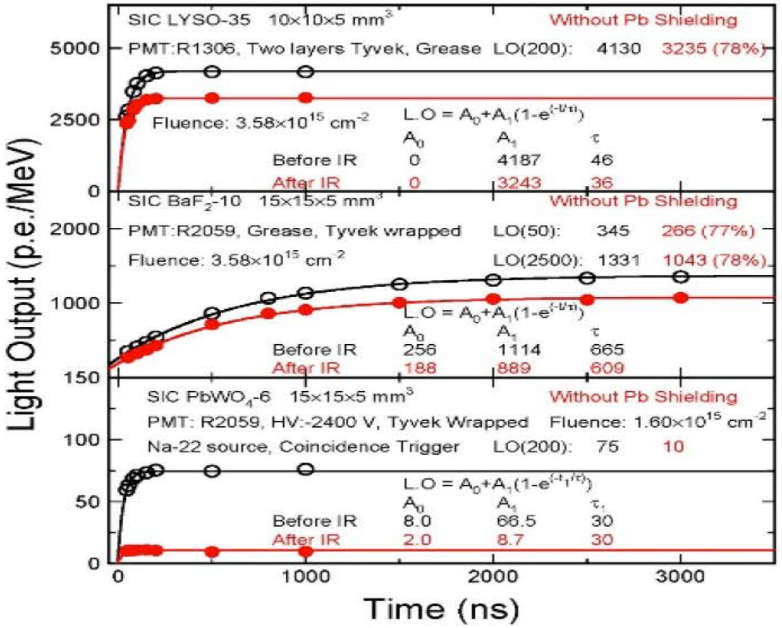

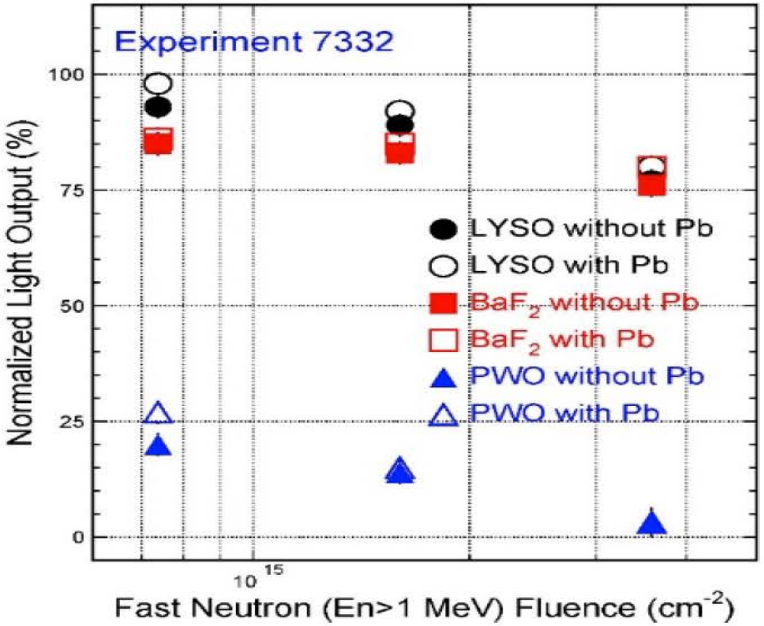

Summary: HEP Experiments

- Commercially available undoped BaF_2 crystals provide sufficient ultrafast light with sub-ns decay time. Yttrium doping in BaF_2 crystals increases its F/S ratio significantly while maintaining the intensity of the sub-ns fast component. With sub-ns pulse width BaF_2:Y is a promising material for the Mu2e-II calorimeter and front imager for GHz hard X-ray imaging.
- 20 cm long BaF_2 crystals are rad hard up to 120 Mrad. Results of the LANL experiments show 800 MeV protons and fast neutrons up to 1×10^{15} p/cm^2 and 3.6×10^{15} n/cm^2 do not cause significant light output loss in 5 mm thick LYSO and BaF_2 plates, promising a very fast and robust detector in a severe radiation environment, such as the HL-LHC.
- Our plan is to further investigate novel ultrafast inorganic scintillators and their radiation hardness. Will also test TPBD WLS for BaF_2:Y, and pay an attention to photodetector with DUV response: LAPPD, Si or diamond etc.

Photek MCP-PMT 110, 210, 240

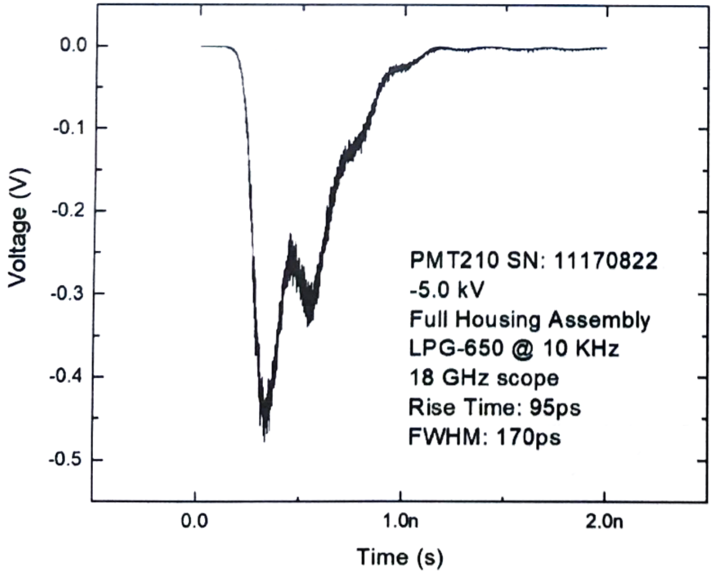

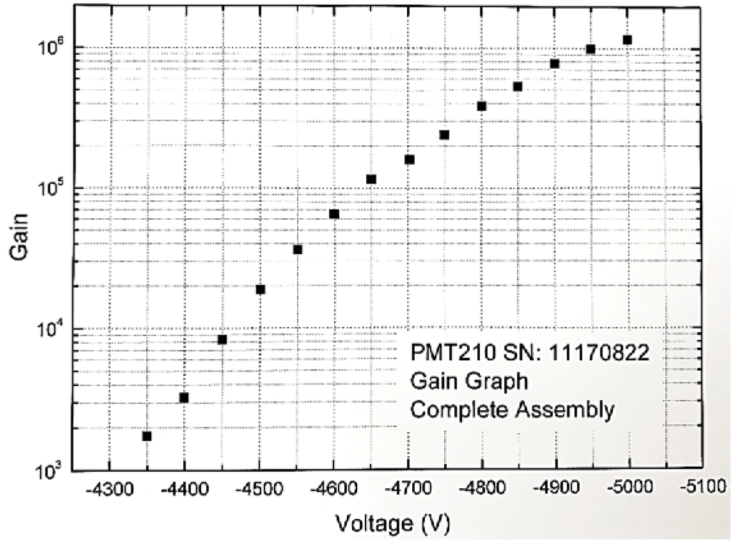

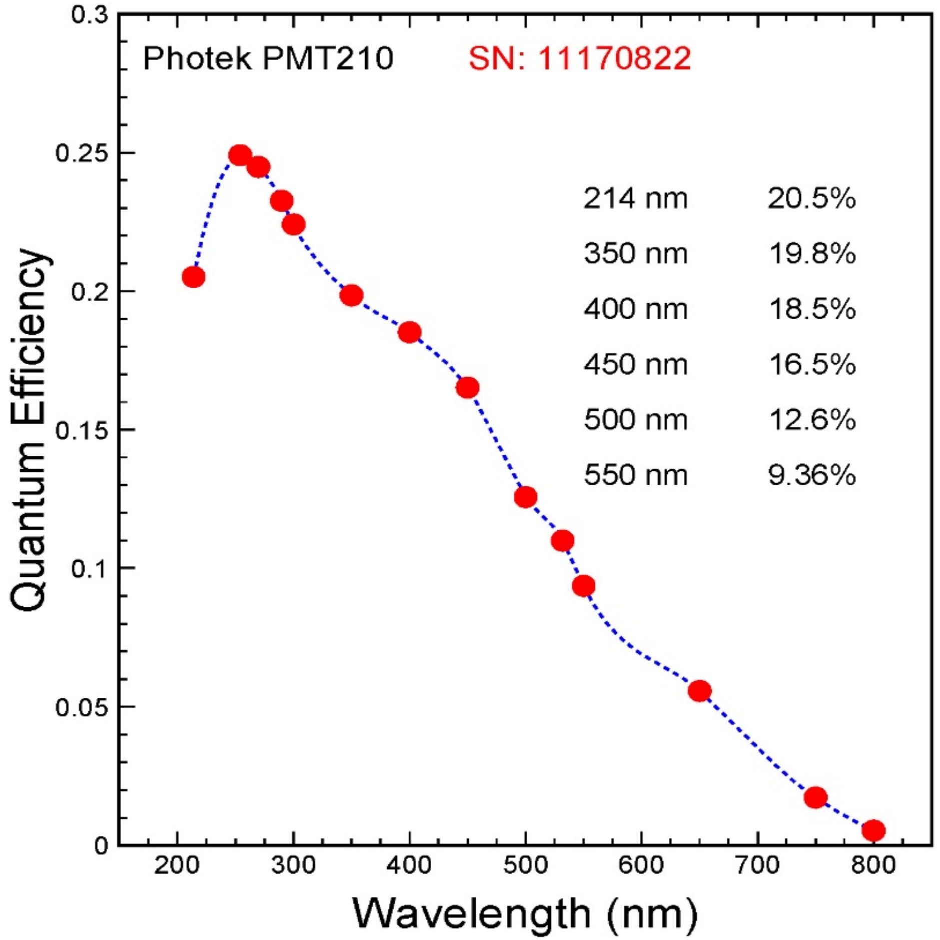

PD	Active area (mm²)	Spectral range (nm)	Peak sensitivity (nm)	Gain	Rise time (ns)	FWHM (ns)
Hamamatsu PMT R2059	Φ46	160-650	450	2×10^7	1.3	3
Photek MCP PMT110	Φ10	160-850	280-450	1×10^4	**0.065**	0.11
Photek MCP PMT210	Φ10	160-850	280-450	1×10^6	**0.095**	0.17
Photek MCP PMT240	Φ40	160-850	280-450	1×10^6	**0.18**	0.85

Hamamatsu S13370 VUV SiPM

VUV-4 has a much better performance than VUV3

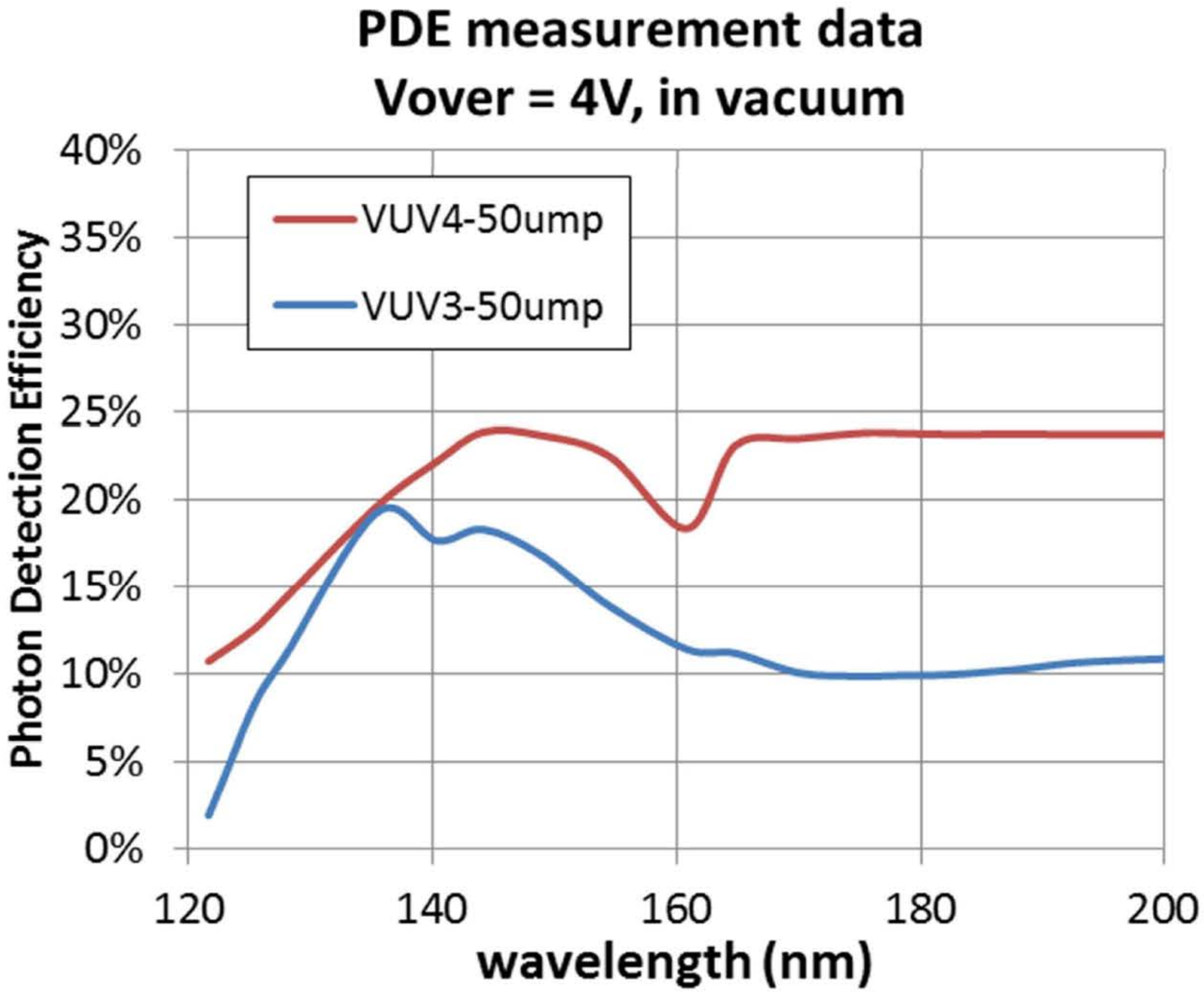

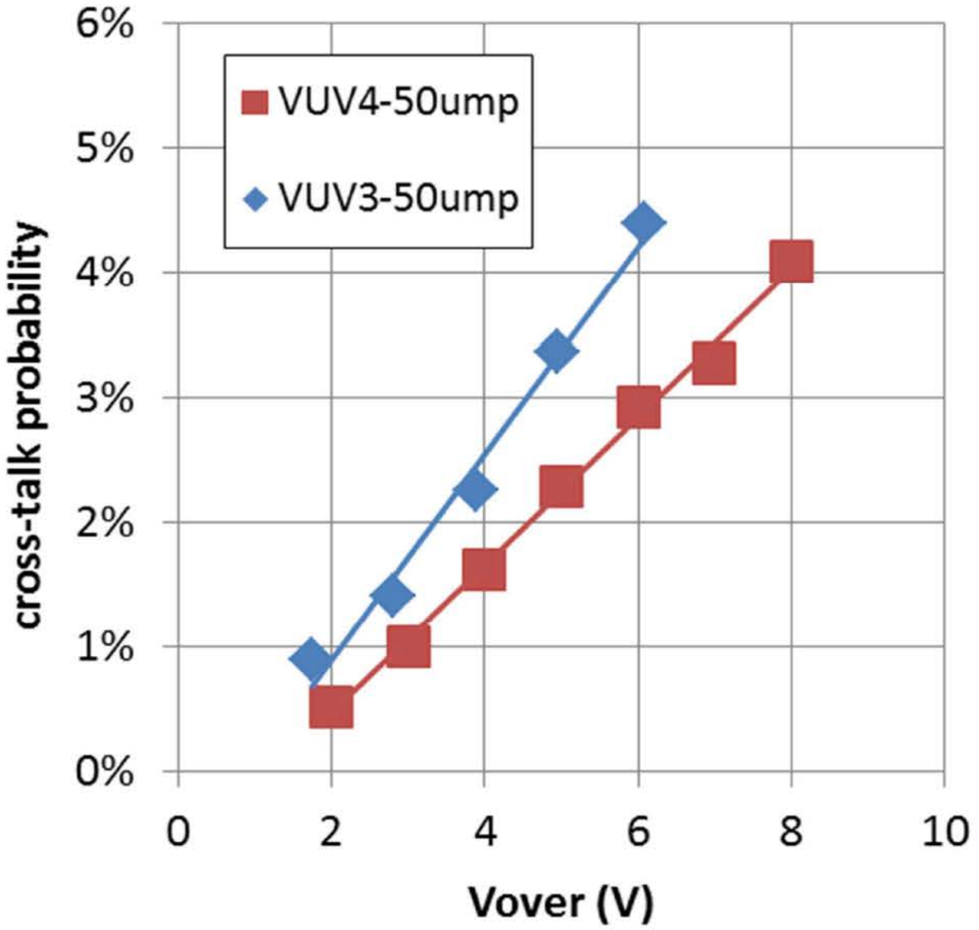

Diamond Photodetector

E. Monroy, F. Omnes and F. Calle,"Wide-bandgap semiconductor ultraviolet photodetectors, IOPscience 2003 Semicond. Sci. Technol. 18 R33

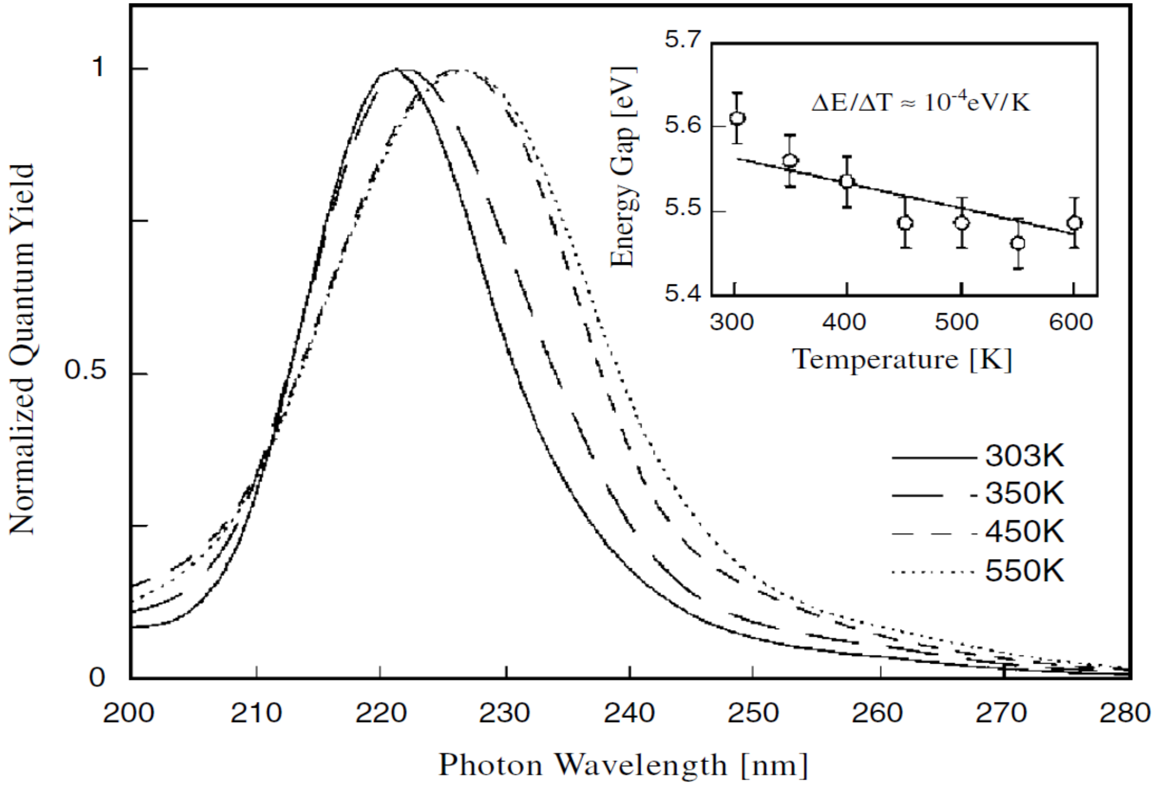

Figure 6. Quantum efficiency of diamond photoconductors at different temperatures and Arrhenius plot of the peak value (inset). (From [Sal00].)

E. Pace and A. De Sio, "Innovative diamond photo-detectors for UV astrophysics", Mem. S.A.It. Suppl. Vol. 14, 84 (2010)

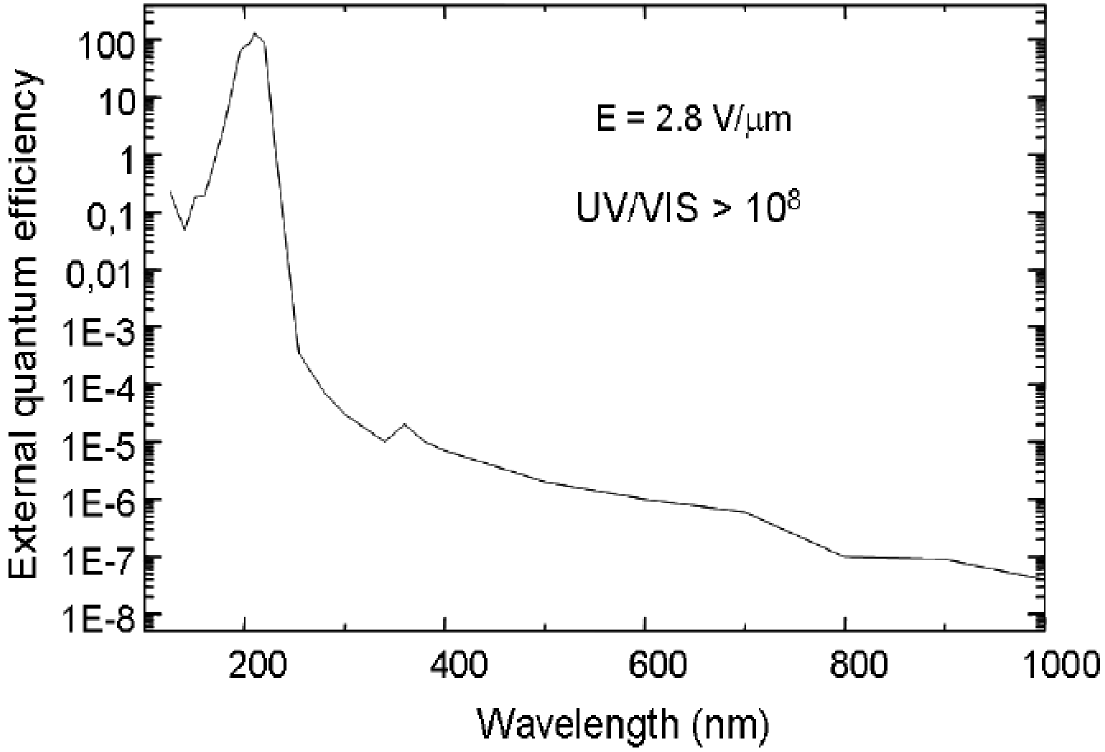

Fig. 4. External quantum efficiency extended to visible and near infrared wavelength regions. The